Title
Enhance osteoinductivity of DBM with Noggin suppression in 3D hydrogel system

Author
Chen, Chen

Publication Date
2020

Peer reviewed|Thesis/dissertation

UNIVERSITY OF CALIFORNIA

Los Angeles

Enhance osteoinductivity of DBM with Noggin suppression in 3D hydrogel system

A thesis submitted in partial satisfaction of the

requirement for the degree Master of Science

in Oral Biology

by

Chen Chen

2020

ABSTRACT OF THE THESIS

Enhance osteoinductivity of DBM with Noggin suppression

in 3D hydrogel system

by

Chen Chen

Master of Science in Oral Biology

University of California, Los Angeles, 2020

Professor Min Lee, Chair

Bone defects have become a challenging health issue after extensive trauma, osteoporosis, and tumor extirpation worldwide [1]. To enhance bone healing, bone grafts have been employed in clinical treatment for many years [2]. Autologous grafts have been considered as the "gold standard" for the bone graft material, but their application is limited by the donor site morbidity [3]. Demineralized bone matrix (DBM), one of the alternations of autologous graft, has been widely used for craniofacial bone repair. However, the application of DBM is compromised due to its rapid dispersion after the implantation and low osteoinductivity [4-7]. In order to deliver and localize DBM, carriers with high bioactivity are in need to be developed.

Chitosan has been proved to be attractive for researchers in the field of tissue bioengineering due to its high biocompatibility, biodegradability, and low immunogenicity [8].

Besides, heparin, a highly sulfated polysaccharide in the extracellular matrix, possesses the typical structure which can interact with multiple osteoinductive factors to enhance and stabilize the biological activities of growth factors [9]. Therefore, we synthesized a chitosan-based hydrogel with heparinized conjugation (Hep-MeGC), which can not only deliver DBM but also enhance its osteogenic activity. Moreover, upon the stimulation of BMPs (major osteogenic factors in DBM), BMP efficacy is significantly reduced due to increased expression of BMP antagonists like Noggin [10-12]. Thus, the potency of BMPs in DBM may be enhanced through Noggin suppression. This study aims to investigate the new method by using Noggin suppression and Hep-MeGC hydrogel to enhance DBM-mediated bone repair.

To suppress Noggin, human bone marrow stem cells (hBMSCs) were transfected with lentiviral particles that encode Noggin-shRNA. The methacrylate glycol chitosan (MeGC) and heparinized chitosan hydrogel (Hep-MeGC) hydrogel, were then prepared to deliver DBM and BMSCs with Noggin-suppression. The effect of DBM and Noggin suppression on osteogenesis was evaluated *in vitro*, and the ability of DBM and Noggin suppression in Hep-MeGC hydrogels to bone regeneration was investigated through *in vivo* study.

Noggin suppression + DBM greatly enhanced the osteogenesis of BMSCs in Hep-MeGC hydrogels, as shown by the increased ALP production, calcium deposition, and expression of osteogenic genes. The mechanistic study showed that Noggin suppression enhanced the DBM-based osteoinductivity through the stimulation of BMP-Smad signals. Detected by microCT and histological/immunohistochemical analysis, the combinational treatment further displayed a robust bone healing capacity in the critical-sized mouse calvarial defect model. To conclude, the incorporation of DBM and Noggin suppression in the Hep-MeGC hydrogel significantly

promoted bone healing.

The dissertation of Chen Chen is approved.

Tara Lyn Aghaloo

Bo Yu

Min Lee, Committee Chair

University of California, Los Angeles

2020

Table of Content

Chapter 1

Introduction

Bone defects caused by trauma, tumor, degenerative disease, and inflammation, which can influence the patients' life quality, remains a substantial health issue worldwide [1, 13]. Operation is the most commonly used method in the current clinic treatment. However, barriers like following systematic disease and the long-period for recovery constrain the treatment [1, 2, 7, 14, 15]. In recent years, researchers have been exploiting effective methods to enhance tissue regeneration by combining the application of bioactive material, osteoinductive factors, and functional cells [16]. Mesenchymal stem cells (MSCs) belong to multipotent progenitor cells capable of self-renewing and differentiating into several specialized cell types. The typical type of mesenchymal stem cell, which has been widely used for bone healing, is the bone marrow stem cells (BMSCs) due to its high osteogenic differentiation ability into osteoblast [17-19]. Herein, we will use BMSCs to demonstrate a new strategy to enhance bone repair.

Bone-graft materials have been employed in clinical treatment for many years to enhance bone healing [20, 21]. Autologous bone grafts are considered as the "gold standard" for graft materials, but their implementation was limited by the availability and donor site morbidity [3, 21]. Demineralized bone matrix (DBM), a promising alternative to autologous graft, is the allograft bone that has been removed the inorganic materials to better expose its inside multiple osteoinductive factors, especially bone morphogenetic proteins (BMPs) [22, 23]. Previous studies reported that with the high biological activity, DBM possesses osteogenesis potential to promote the differentiation capacity of BMSCs, and has been increasingly used in orthopedics and oral maxillofacial surgery for bone reconstruction [4-6, 24-27]. However, the

implementation of DBM is compromised due to the rapid dispersion of DBM powder, difficulties in handling, and unpredictable osteogenic activity [28] [29-33]. With these barriers, we came up with a resolution to employ the bioactive carriers to localize and stabilize DBM in the target region.

Currently, the available commercial delivery systems for DBM are the liquid carriers, but they are of weak resistance to irrigation, eliminating the efficacy for osteogenesis in bone defects [34, 35]. Hydrogels, as the polymer network materials, have already been widely applied in delivering drugs, cells, and growth factors for tissue engineering, and with the porous structure, they can regulate the release of the encapsulated materials. The injectable biopolymer-hydrogels with biological compatibility can be degraded by the enzymes in the body or integrate with nearby tissue, preventing the repeated invasive operation from removing the delivery material [36, 37]. Chitosan, as the natural polymer, is highly pursued when designing the injectable hydrogel due to its attractive biocompatibility and hydrophilic characteristics [8, 38]. Our lab previously designed a series of photopolymerizable chitosan-based hydrogels which exhibited high biocompatibility and possessed a promising capacity to deliver and localize the stem cells and growth factors to enhance tissue regeneration [39-44]. The methacrylate glycol chitosan (MeGC) hydrogel possesses the ability to be functionalized through various modifications on the abundant amino groups to enhance biomineralization [43]. Moreover, heparin belonging to the sulfonated polysaccharides can stabilize and interact with multiple osteoinductive factors like BMPs due to its high affinity towards N-terminal domains of BMPs [44-47]. Also, heparin stabilizes BMP by affecting its binding to the type-II receptor subunit and assisting the dimerization of the type-II receptor on cells [48]. With the strong

negative charged group, heparin also interacts with growth factors with a positive charge, like BMPs, and better control their release from the delivery material [49]. Therefore, we proposed that the employment of the chitosan-based hydrogel with heparin conjugation (Hep-MeGC) can localize and enhance the osteogenic activity of DBM.

Moreover, the significant osteoinductive commitment of DBM mainly comes from the inside BMPs (the major osteoinductive factors). Upon the stimulation of BMPs, the efficacy of BMPs can be reduced due to the increased expression of BMP antagonists. Noggin, one of the antagonists of BMP, of which expression can be induced by the increased level of BMPs, negatively regulates the expression of BMPs in cells of the osteoblast lineage [11]. Having a high affinity towards the receptors of BMPs, Noggin can reduce the BMP signaling by binding to their receptors competitively [10-12, 50]. Previous studies have demonstrated that the reduction of Noggin can enhance osteogenesis *in vitro* and bone formation *in vivo* [51, 52]. We suggested that the potency of BMPs in DBM may be increased through abrogating the antagonism, and Noggin suppression can further enhance the osteogenic activity of DBM.

Together, we hypothesize that the strategy of Noggin-suppression and Hep-MeGC hydrogel can enhance the DBM-mediated bone repair. This concept will be evaluated through *in vitro* and *in vivo* study. Briefly, the osteogenic effects of DBM and Noggin-suppression on BMSCs will be examined in both MeGC and Hep-MeGC hydrogel *in vitro*. The critical-sized mouse calvarial defect model (n=6 defects/group) will be used for in vivo experiment. The extent of bone healing will be measured by the microCT images/quantification, histology analysis, and immunohistochemical staining. Mechanistically, we will also investigate whether Noggin-suppression enhances the osteogenic activity of DBM through BMP-Smad signaling. Such the

complementary strategy may build a solid foundation for the broad bone-related regeneration in the future clinical treatment.

Chapter 2

Materials and Methods

2.1 Cell culture

Human bone marrow stem cells (hBMSCs) were purchased from American Type Culture Collection (ATCC, Manassas, VA). In the 37°C and 5% CO2 humidified environment, cells were incubated in growth medium which consists of high glucose Dulbecco's Modified Eagle's Medium (DMEM, Life Technologies, Grand Island, NY), 1% (v/v) penicillin/streptomycin (AA, Life Technologies), and 10% (v/v) fetal bovine serum (FBS, Mediatech Inc, Manassas, VA).

2.2 Noggin knockdown through gene transduction

To suppress Noggin in BMSCs, cells were transfected with lentiviral particles encoding Noggin-shRNA (Santa Cruz, Dallas, TX) following the instruction protocols, and the negative control cells were established after the transfection with the lentiviral particles encoding scrambled shRNA. Briefly, cells were seeded in a 6-well plate, treated with the target shRNA lentiviral particles and polybrene at 70% confluency and incubated overnight. Puromycin dihydrochloride selection was employed to select the clones with stable expression of shRNA. Control and Noggin-suppression BMSCs were collected separately for the following experiments.

2.3 Preparation of the MeGC and Hep-MeGC hydrogels

Glycidyl methacrylate was added in glycol chitosan solution dissolved in distilled water (2% w/v) to obtain a 1:1.1 M ratio solution. The PH of the mixture was adjusted to 9.0 with 0.1N HCl and reacted for 48h on the gentle shaking bed at room temperature. After being

dialyzed with 50 kDa dialysis tubes against distilled water for 1 day, the purified MeGC solution was frozen and lyophilized for at least 48h [41-44]. MeGC was dissolved in 1x phosphate-buffered saline (PBS) to obtain the 2% MeGC hydrogel.

In order to prepare the heparinized glycidyl methacyrlated chitosan (Hep-MeGC) hydrogel, 1-ethyl-3-(3-dimethyl- aminopropyl)-carbodiimide (EDC) was dissolved in the distilled water and reacted with heparin for at least 30 minutes on gentle shaking bed under the room temperature. The solution was mixed with 1% MeGC for 12 hours, dialyzed for 16 hours with 50 kDa tubes and lyophilized for 48 hours. The Heparinized chitosan was later dissolved in 1x PBS to obtain 2% (w/v) Hep-MeGC hydrogel for further experiment.

2.4 Cell and DBM encapsulation by the photopolymerizable hydrogel

BMSCs were encapsulated in the hydrogel with the concentration of $2x10^6$ cells/ml in the presence and absence of DBM (Musculoskeletal Transplant Foundation biologic). The photopolymerizable hydrogel was initiated by 6 μM riboflavin initiator (100:0.5 vol ratio) and formed after the irradiation of visible blue light for 40 seconds (VBL, 400–500nm, 300 mW/cm^2, Bisco Inc., Schaumburg, IL). BMSCs encapsulated by hydrogel were cultured in 1ml growth medium in 37°C and 5% CO_2 environment condition.

2.5 Western blot

Proteins were extracted from BMSCs in a 6-well plate by RIPA lysis buffer (EMD Millipore Corp., Billerica MA, USA), and the protein concentration was determined by a BCA assay kit (Thermo Scientific). Protein samples were loaded on 10% SDS-PAGE gel and were initially separated in Tris/glycine/SDS running buffer (Bio-Rad) at 90V in top gel then changed into 120V after reaching the bottom gel. Proteins were transferred onto the immobilon transfer

membrane (Merck Millipore Ltd.) at 250V, 260mA for 120 min. After blocking with 5% non-fat milk at 4°C overnight, the membrane was washed with PBS/T (PBS with 0.1% Tween-20). Primary antibodies against Noggin, Smad 1/5/8, and GAPDH (Santa Cruz) were diluted with PBS/T and incubated with the blocked membrane for 2h. Following the wash of PBS/T, membranes were incubated with the second antibodies (diluted by PBS/T with 5000:1vol ratio) and incubate the membrane for 1h at room temperature. The Clarity Western ECL Substrate (Bio-Rad) was utilized to detect the signal. The membrane was incubated at room temperature for 60 seconds with reagents and exposed to the western workflow (Bio-rad). Images were demonstrated by ImageLab software (Bio-Rad), and the quantification was performed by ImageJ software.

2.6 Cell proliferation in hydrogel

The proliferation of encapsulated BMSCs in the hydrogel was measured by Alamar blue assay kit (Bio-Rad, CA, USA). Briefly, hydrogels were incubated in 10% (v/v) Alamar blue reagent for 3h, and fluorescence was measured at 530 (excitation) and 590 (emission) nm. Besides, live/dead fluorescence staining was employed to detect the viability and morphology of the encapsulated cells in the hydrogel. hydrogels were stained with calcein and ethidium homodimer by using live/dead assay kit (Invitrogen, Carlsbad, CA) for 15min under 37°C and 5% CO2 environment. The fluorescence was observed by an Olympus IX71 fluorescence microscope (Olympus, Tokyo, Japan).

2.7 Alkaline phosphatase (ALP) and ALP activity

For the 2D experiment, BMSCs were cultured in a 12-well plate with a density of 15,000 cells/well in the growth medium. After arriving at 90% confluency, the growth medium was

replaced by the osteogenic medium, which was supplemented with 50 μg/ ml L-ascorbic acid, 10 mM b-glycerophosphate, and 100 nM dexamethasone (Sigma) to the growth medium. In the 3D environment, the hydrogels loading with cells and DBM were initially cultured in growth medium during the first day and transferred to the osteogenic medium on the second day. To detect the osteogenic differentiation capacity of the cells, ALP production was examined through ALP staining and it protein activity tests. Briefly, samples were initially fixed with 10% formalin at room temperature, washed with phosphate-buffered saline (PBS) twice and incubated in ALP staining solution which was made of 5-Brom-4-chlor-3 indoxyl phosphate (BCIP, Sigma) and Nitro Blue tetrazolium (NBT, Sigma) stock solutions in AP buffer for 2h. After the staining, images were observed by the Olympus IX71 microscope (Olympus, Tokyo, Japan). To further qualify the protein activity, hydrogels were incubated in 0.1% Tween-20 for digestion. P-Nitrophenol phosphate was then utilized to assess the absorbance at 405nm. The total protein concentration was tested through the Pierce BCA assay kit (Thermo Scientific, Rockford, IL) to normalize the result [53, 54].

2.8 Alizarin red S staining and quantification

The backward stage of osteogenic differentiation in BMSCs moves the calcium deposition. Alizarin red S staining and its quantification was performed on day 21 to investigate the mineralization. After being fixed by 10% formalin, hydrogels were stained with 2% Alizarin red S solution for 30 min and washed with PBS for 2h on the gentle shaking bed. Images were captured and observed by using the Olympus IX71 microscope (Olympus, Tokyo, Japan) [53, 54]. The stained samples were then quantitatively analyzed through dissolving the stained composites in 10% (v/v) acetic acid, followed by assessing the absorbance at 405 nm [42, 53,

54].

2.9 Real-time quantitative polymerase chain reaction (qRT-PCR)

To investigate the RNA expression of the osteogenic genes in BMSCs, total RNA was extracted by Trizol (Life Technologies) and purified by RNeasy Mini Plant kit (Qiagen, Valencia, CA). RNAs were then transcribed into cDNA. The gene expression was measured after the amplification. GAPDH was employed to normalize the expression of the target genes. Experiments were performed in triplicate. Sequence of primers for real-time PCR assay are listed below.

Noggin-F	ATCGAACACCCAGACCCTATC
Noggin-R	TCTAGCCCTTTGATCTCGCTC
BMP2-F	GGCACTGGGATGTCTACTCTA
BMP2-R	CCATCACAGATAGCAACCTGACT
Smad5-F	CCAGCAGTAAAGCGATTGTTGG
Smad5-R	GGGGTAAGCCTTTTCTGTGAG
ALP-F	ATGGGATGGGTGTCTCCACA
ALP-R	CCACGAAGGGGAACTTGTC
Runx2-F	ATTCCTGTAGATCCGAGCACC
Runx2-R	GCTCACGTCGCTCA TTTTGC
GAPDH-F	ATGGGGAAGGTGAAGGTCG
GAPDH-R	GGGGTCATTGATGGCAACAATA

2.10 Histology section with H&E staining

BMSCs and DBM were encapsulated in the hydrogel and the composites were cultured in

the growth medium over a duration. Hydrogels were collected and were fixed with 10% formalin on day 1 and day 14, respectively. After being embedded in paraffin and cut into 7μm section, the sections were stained with hematoxylin and eosin to demonstrate the distribution and morphology of the encapsulated cells. Sections were observed by the Olympus IX71 microscope (Olympus, Tokyo, Japan).

2.11 Animal care

All of the animal experiment procedure was practiced strictly under the supervision and approved by Chancellor's Animal Research Committee of the Office for Protection of Research Subjects at UCLA and follow the instruction of the UCLA Office of Animal Research Oversight. The adult nude mice between 8-12weeks old were purchased from Charles River Laboratories (Wilmington, MA) (n = 3-4 in each group) and were cared under the direction of the Guidelines for the Care and Use of Laboratory Animal of the National Institutes of Health [43, 55, 56].

2.12 Calvarial Defect Model

After being anesthetized, a critical 3-mm full-thickness calvarial defects were created on parietal bone in mice with the trephine drill. 30μl MeGC hydrogels encapsulating control or Noggin-suppression hBMSCs in the presence and absence of DBM were placed in each of the defect regions. After the surgery, all of the experiment mice could be allowed to fully recover from anesthesia and then transported to the vivarium for later care. As for the post-operation treatment, all mice were injected with buprenorphine (0.1 mg/kg) up to 3 days and got drinking water with trimethoprim-sulfamethoxazole for 7 days to prevent infection [43, 55, 56].

2.13 Micro-computerized tomography (μCT) scanning

Calvarial tissues were collected from mice after 6 weeks of the operation. The extracted tissues were fixed with 4% formaldehyde for 48h at room temperature and rinsed with PBS. All of the samples were immersed in 70% ethanol before taking images with a high–resolution MicroCT machine (μCT40; SkyScan 1172; SkyScan, Kontich, Belgium) with 57 kVp, 184 μA, 0.5 mm aluminum filtration and 10μm resolution. The reconstruction of the 3D structure was done by Dolphin 3D software (Dolphin Imaging & Management Solutions, CA), and the Image J software (NIH, Bethesda, Maryland) was employed to evaluate the defect size [43, 55, 56].

2.14 Histological Evaluation

After being scanned by micro CT, samples were kept in 10% EDTA solution under room temperature on the gentle shaking bed for 1 week and embedded in paraffin for section and later staining, including hematoxylin and eosin (H&E), Masson-Goldner trichrome (MGT) and Picrosirius red staining. Sections were observed using the Olympus IX71 microscope (Olympus, Tokyo, Japan).

As for the immunohistochemistry, slides were stained to detect the expression of osteogenic differentiation genes, OCN. Briefly, after being processed with citric acid antigen retrieval, slides were incubated in the first antibody of OCN (Santa Cruz Biotechnology, CA) and stained by HRP/DAB detection kit (Abcam, MA) [43, 55, 56].

2.15 Statistical analysis

All of the experiments are performed in triplicate, and all the values presented in this thesis were represented by the average number. P-value<0.05 was considered significant, and the error bars represented the standard deviation. One-way analysis of variances (ANOVA) was utilized to do statistical analysis.

Chapter 3

Noggin-suppression and DBM enhances osteogenesis BMSCs by stimulating BMP-Smad signaling

3.1 BMP-2 released from DBM

DBM has been proved to be a promising and satisfactory bone graft material with extensive utilization as a commercial product providing a potential delivery system for multiple osteoinductive factors like BMPs to produce dose-dependent osteogenesis [25-27, 57-59]. In order to investigate the release rate of the BMP-2 (major osteoinductive factor in DBM), DBM was incubated in the osteogenic medium for 14 days (40mg/ml), and the supernatant was collected on day 1, day 4, day 7 and day 14 for Elisa assay (Figure 3.1). Results showed that the accumulative concentration of BMP-2 reached a peak on day 7.

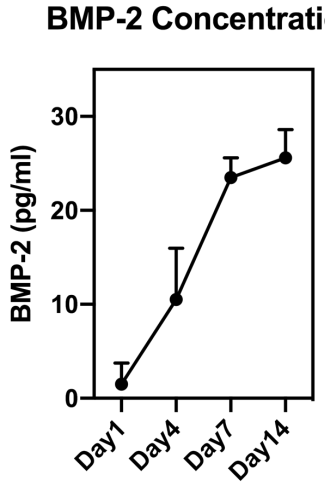

Figure 3.1. DBM was incubated in the osteogenic medium with a concentration of 40mg/ml for 14 days. ELISA was conducted to evaluate accumulative BMP-2 concentration released from DBM in the supernatant collected on day 1, 4, 7, and 14.

3.2 DBM induces Noggin expression in BMSCs

To determine an optimal concentration of the DBM, which could efficiently enhance the osteogenic differentiation of BMSCs, DBM was incubated in osteogenic medium with various concentrations (0-40mg/ml), and the supernatant was collected on day 7 to treat BMSCs. The differentiation ability of BMSCs into osteoblasts could be examined by ALP expression through ALP staining and its activity test. The most intensified staining was observed in BMSCs treated with 3mg/ml DBM supernatant, indicating the practical differentiation ability (Figure 3.2).

Noggin, the ligand-binding type antagonist of BMP, negatively regulates the increased level of BMPs. To investigate the expression of Noggin in BMSCs, which was induced by the treatment of DBM (3mg/ml), qRT-PCR and western blot was carried out after 48 hours. As a parallel comparison, cells were also cultured in BMP-2 (diluted with osteogenic medium with a concentration of 300ng/ml). The application of DBM or BMP-2 both induced the RNA expression of Noggin in BMSCs compared with the non-treated control (Figure 3.3A). Consistent results from the western blot and its quantification also demonstrated that the implementation of DBM or BMP-2 exhibited the powerful ability to induce Noggin expression (Figure 3.3B).

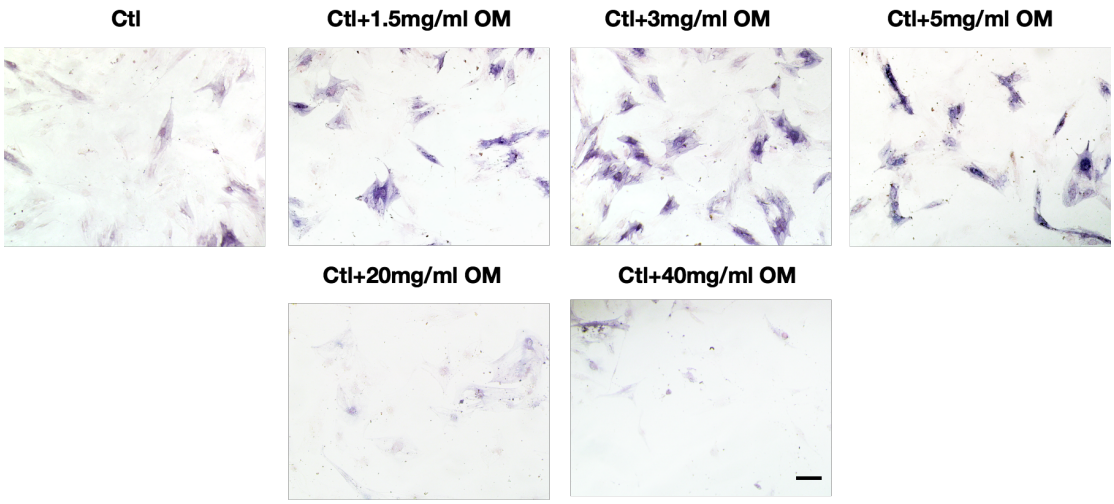

Figure 3.2. DBM (0-40 mg/ml) was incubated in osteogenic medium for 7 days and the supernatant was collected to treat cells for ALP staining on day 4 (Scale bar=200 μm).

A

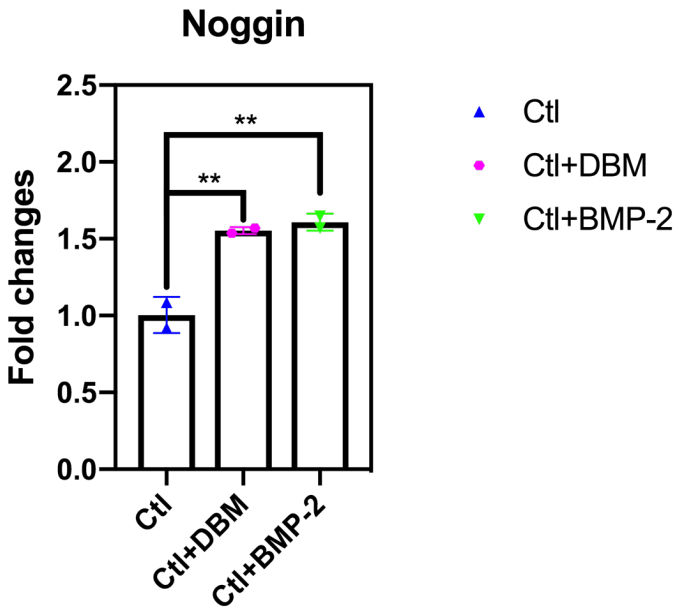

B

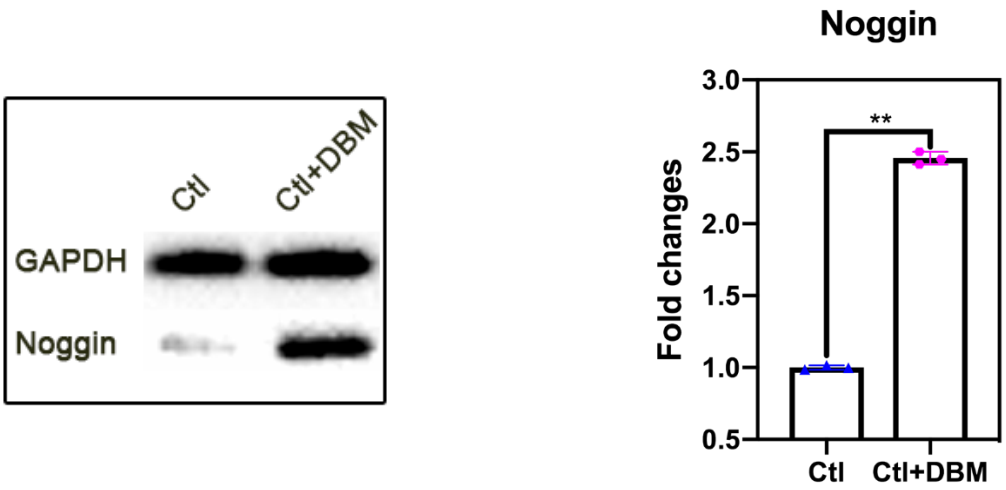

Figure 3.3. DBM was incubated in the osteogenic medium (3mg/ml), and the supernatant was collected on day 7. BMSCs were respectively treated with the DBM supernatant and BMP-2 (diluted in osteogenic medium with the concentration of 300ng/ml) for 48 hours. The expression of Noggin was evaluated through qRT-PCR (A); and western blot(left). The quantification was conducted by using Image J software (right) (**P<0.05).

3.3 Noggin-suppression enhances the osteogenic activity of DBM

To suppress Noggin, BMSCs was transfected with the lentiviral particles encoding Noggin-shRNA. The effect of Noggin suppression and DBM on osteogenesis of BMSCs was evaluated by detecting the ALP production and the expression of the osteogenic gene. With the application of DBM, Noggin suppression increased ALP activity to 2.49-fold when compared with the non-treated control (Figure 3.4). qRT-PCR was conducted to examine the RNA expression of Noggin and specific osteogenic genes. The application of DBM enhanced the expression of Noggin in both control and Noggin-suppression BMSCs. In the Noggin-suppression BMSCs, DBM increased the expression of Runx2 and ALP to 3.40-fold and 5.54-fold, respectively, which is significantly higher than that in the control cells (Figure 3.5). All results confirmed that the Noggin-suppression strategy enhanced the osteogenic activity of DBM, and the combined method of Noggin-suppression + DBM possess the efficient ability to improve the osteogenic differentiation of BMSCs.

A

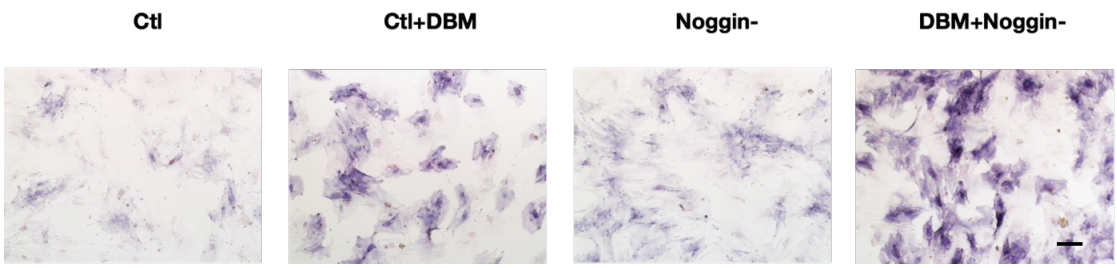

B

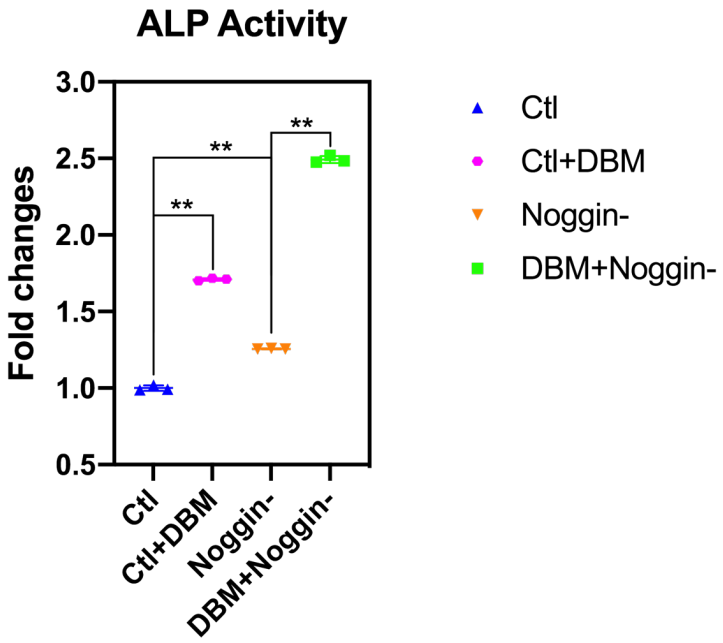

Figure 3.4. BMSCs were cultured in the osteogenic medium and DBM supernatant (3mg/ml), respectively. ALP staining (A) and ALP activity were examined on day 7 (B). (**P<0.05; Scale bar=200 μm)

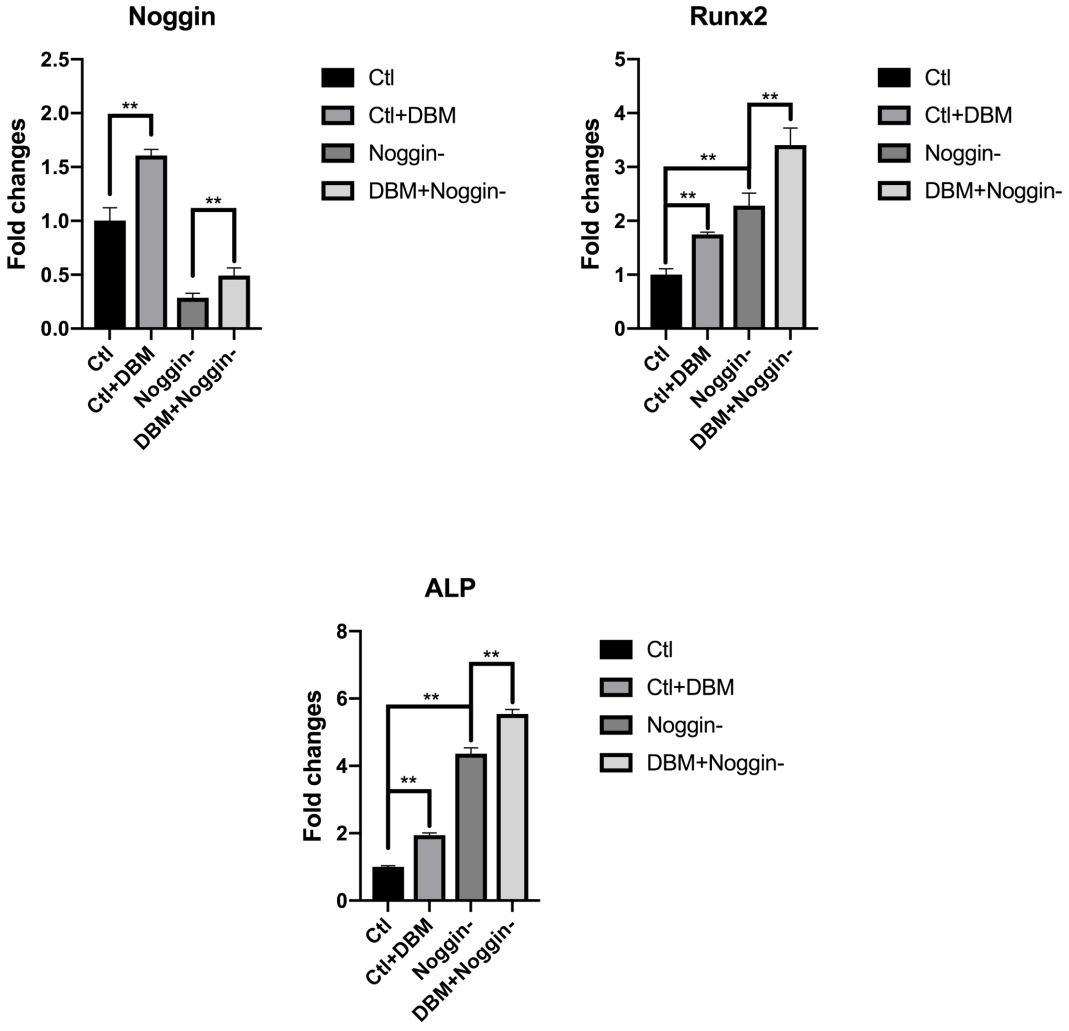

Figure 3.5. Control and Noggin-suppression BMSCs were cultured in the osteogenic medium and DBM supernatant (3mg/ml) respectively. The RNA expression of Noggin, Runx2 and ALP was investigated after 48 hours of induction through qRT-PCR (**P<0.05).

3.4 Enhanced osteogenic differentiation of DBM and Noggin suppression by stimulating BMP-Smad signaling

The regulatory mechanism of molecular signaling through which the Noggin-suppression enhances the osteoinductivity of DBM was investigated. qRT-PCR was employed to evaluate the RNA expression of the BMP-related components for BMP-Smad signaling in BMSCs after 48 hours of the osteogenic induction. When compared with the non-treated control, Noggin-shRNA transduction and DBM increased the expression of BMP-2 and Smad-5 in BMSCs to 2.73-fold and 3.05-fold (Figure 3.6A). In the translational level, the expression of Noggin and specific BMP-related protein, Smad 1/5/8, was evaluated through western-blot assay and its quantification. DBM significantly induced the expression in Noggin in both control and Noggin-suppression BMSCs. With the implementation of DBM, a distinct elevation in Smad 1/5/8 expression was shown in the Noggin-suppression BMSCs, confirming that Noggin suppression enhanced the osteogenic activity of DBM by stimulating BMP-Smad signals (Figure 3.6B).

A

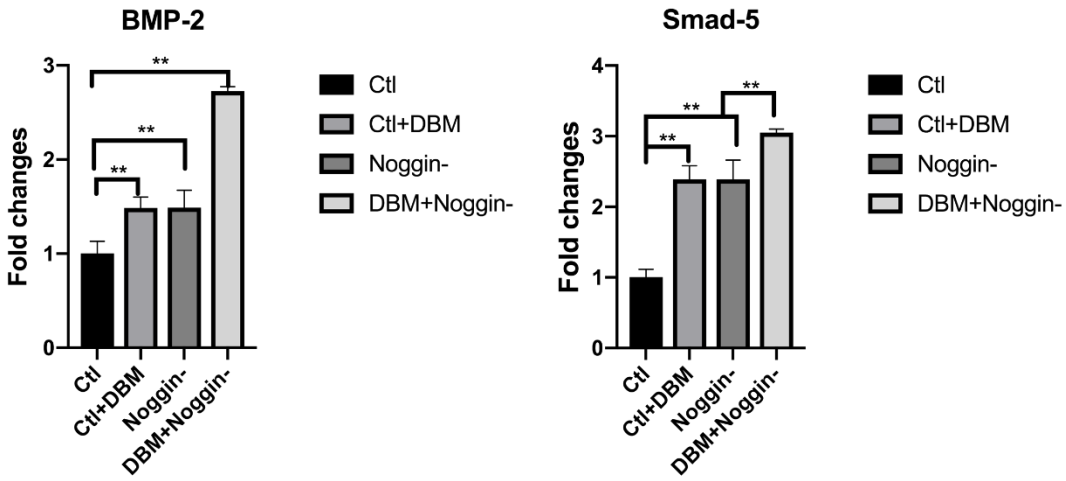

B

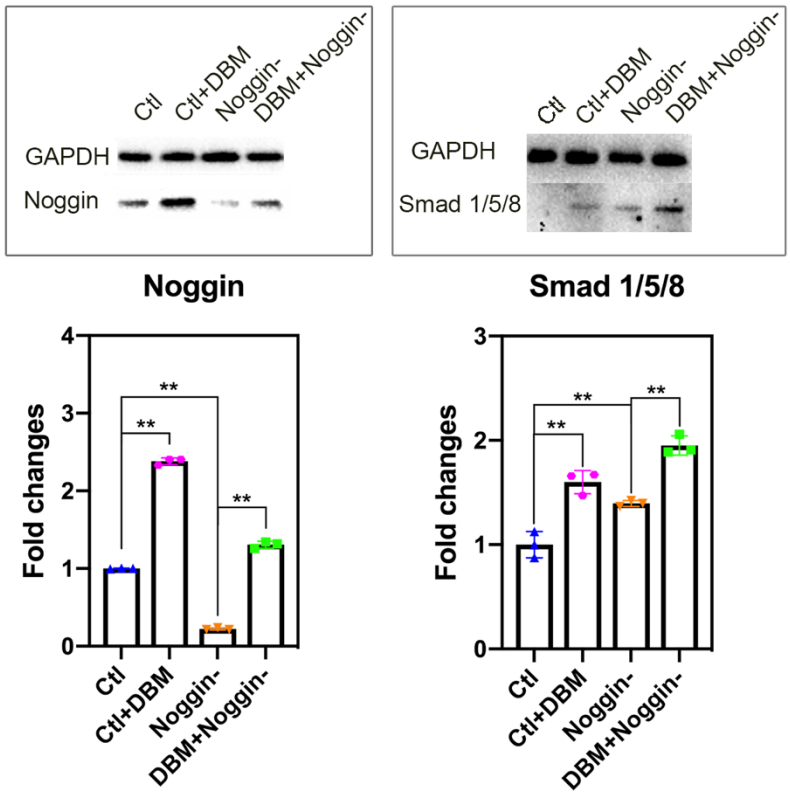

Figure 3.6. BMSCs were cultured in DBM supernatant (3mg/ml) and osteogenic medium, repsectively. qRT-PCR was employed after 48 hours' incubation to detect BMP-2 and Smad-5 expression(A). The protein expression of Noggin and Smad 1/5/8 were characterized by Western blot, and qualifid by Image J Software (B) (**P<0.05).

Chapter 4

Hydrogel delivers DBM with Noggin suppression

4.1 MeGC hydrogel delivers DBM and BMSCs

As the delivery system, the visible light cross-linkable chitosan hydrogel (MeGC) fabricated with riboflavin initiator (RF) was prepared, and DBM along with BMSCs (with the concentration of $2x10^6$ cells/ml) were homogenously co-encapsulated in the hydrogel for the following 3D study. To determine the optimal DBM to hydrogel ratio, which could significantly promote the differentiation of the encapsulated cells, MeGC hydrogel integrated with DBM to form DBM-hydrogel composites with various weight ratios (0/1-2/1). The osteogenesis of the BMSCs in the hydrogel was evaluated by detecting the expression of ALP, the early osteogenic marker, through ALP staining on day 7. The DBM-hydrogel composite with 1/1 ratio increased the ALP activity to 1.86-fold, which is notably higher than that detected in other ratios (DBM/hydrogel depends on the ratio of the components on a dry weight basis) (Figure 4.1).

A

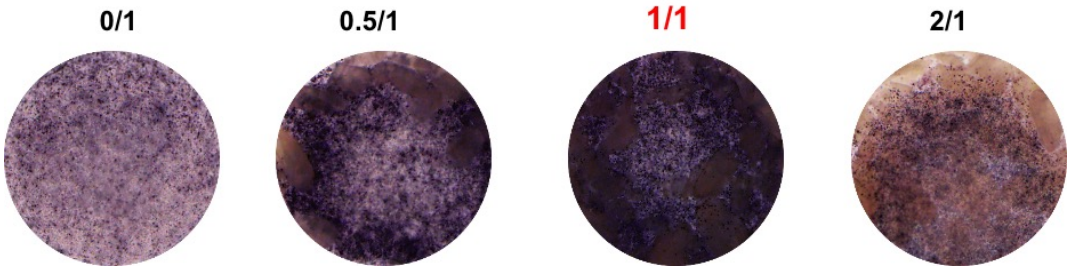

B

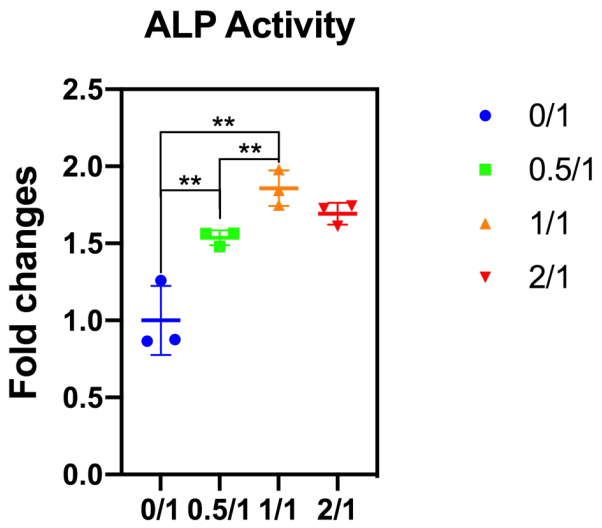

Figure 4.1. BMSCs and DBM were encapsulated in the MeGC hydrogel with different DBM/hydrogel ration (0/1-2/1). ALP staining (A) and ALP activity test (B) were carried out to characterize the osteogenic differentiation of BMSCs on day 7 (DBM/hydrogel depends on the ratio of the components on a dry weight basis; (**P<0.05).

4.2 BMSCs proliferation in the MeGC hydrogel with Noggin suppression and DBM

With the selected DBM to hydrogel ration (1/1), BMSCs and DBM were seeded in the MeGC hydrogel to investigate the morphology changes and proliferative potential of the encapsulated cells. Images from live/dead fluorescence staining showed that both control and Noggin-shRNA treated BMSCs maintained viability and spread alongside the DBM in MeGC hydrogel (Figure 4.2A). Histology section with hematoxylin and eosin (H&E) staining was performed to characterize the distribution of the BMSCs and DBM. BMSCs stained with purple color gathered into clusters and lacunae alongside DBM, suggesting that DBM is attractive to the co-encapsulated cells (Figure 4.2B). Hematoxylin staining represented the formation of basophilic substance, and eosin staining demonstrated the eosinophilic component. The proliferation of the BMSCs in the MeGC hydrogel was evaluated by Alamar blue assay. Continuous elevations of the fluorescence intensity were observed over 14 days (Figure 4.2C).

A

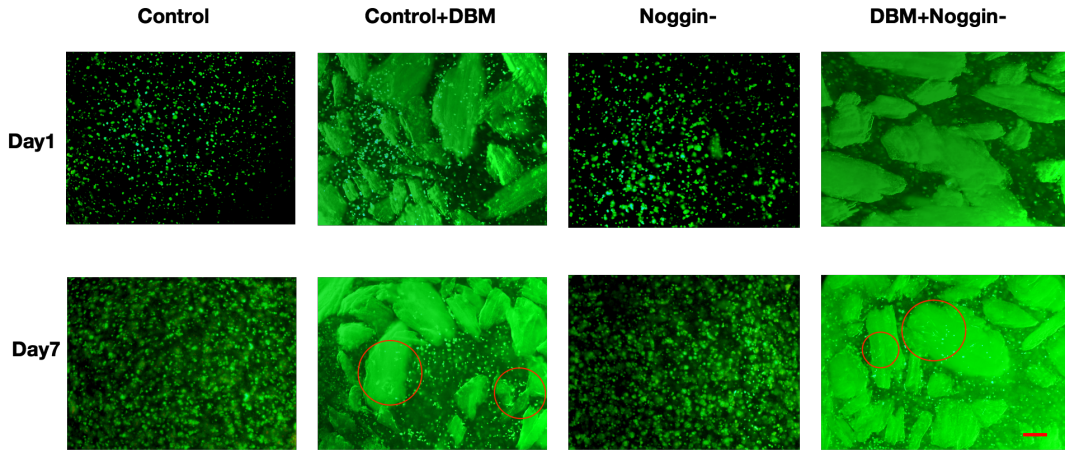

B

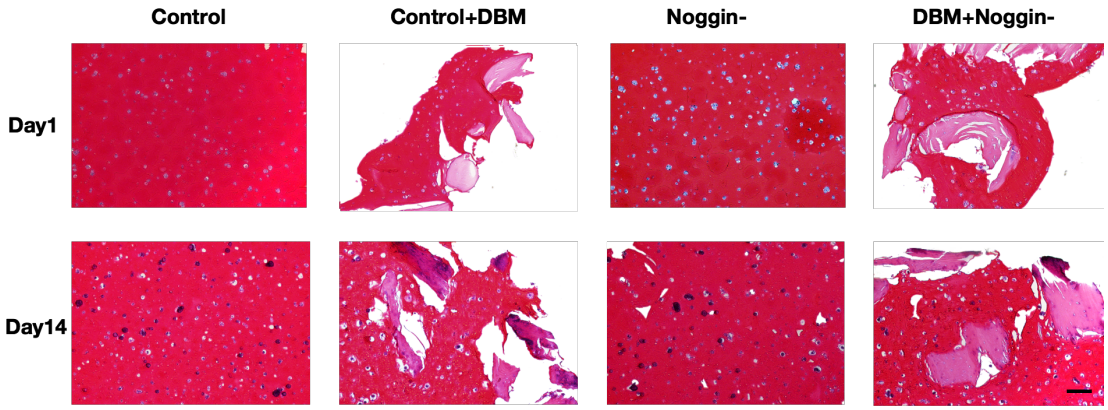

C

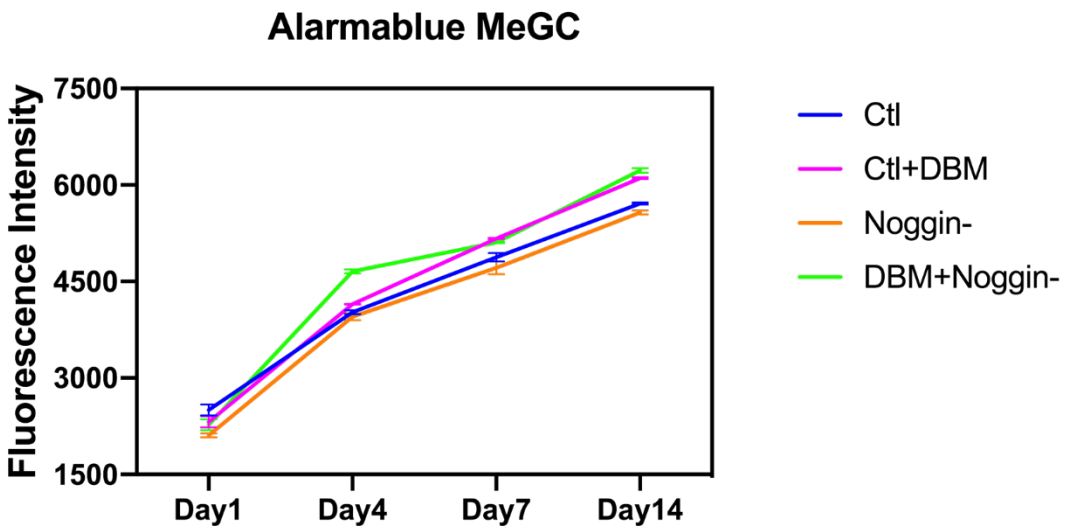

Figure 4.2. The distribution and morphology changes of the encapsulated BMSCs in the MeGC hydrogel was exhibited through live/dead fluorescent staining on day 1 and day 7 (A); histology section with H&E staining on day 1 and day 14 (B). The proliferation potential was investigated through Alamar blue assay over 14 days (C) (Scale bar=500 μm)

4.3 Osteogenesis of BMSCs in the MeGC hydrogel with Noggin-suppression and DBM

The expression of ALP evaluated the osteogenic differentiation of the encapsulated BMSCs with Noggin suppression and DBM in the MeGC hydrogel. Results from ALP staining showed the most intensified color in the hydrogels loaded with Noggin-suppression BMSCs and DBM (Figure 4.3A). The application of DBM significantly increased the value of ALP activity to 1.28-fold in the control cells, and the Noggin-shRNA transfection extensively enhanced the protein activity to 1.72-fold (Figure 9B). The expression of the osteogenic gene markers can also be employed to investigate the differentiation of the BMSCs through qRT-PCR. The Runx2 and ALP expression were increased to 2.04-fold and 2.46-fold with the Noggin suppression, and the stimulation of DBM further enhanced the expression to 3.16-fold and 3.06-fold, when compared with control BMSCs. (Figure 4.3C).

The calcium deposition characterized the backward stage of the osteogenic differentiation in the MeGC hydrogel through Alizarin red S staining and its quantification on day 21. The most intensified staining was observed in the hydrogel with DBM and Noggin-suppression, and the quantification also demonstrated the highest value with the 1.62-fold increase in the ultimate mineralization, confirming the distinct escalation of osteogenic differentiation (Figure 4.4).

Together, demonstrated by the increased ALP production, mineralization, and the expression of the osteogenic gene, Noggin-suppression possesses the promising potential to enhance the osteogenic activity of DBM in MeGC hydrogel.

A

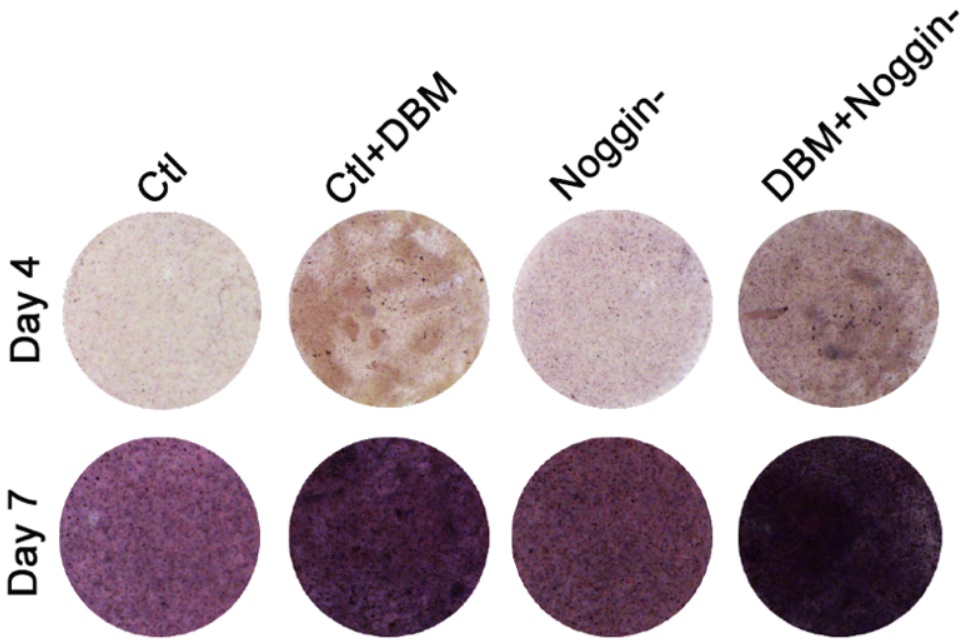
Ctl
Ctl+DBM
Noggin-
DBM+Noggin-
Day 4
Day 7

B

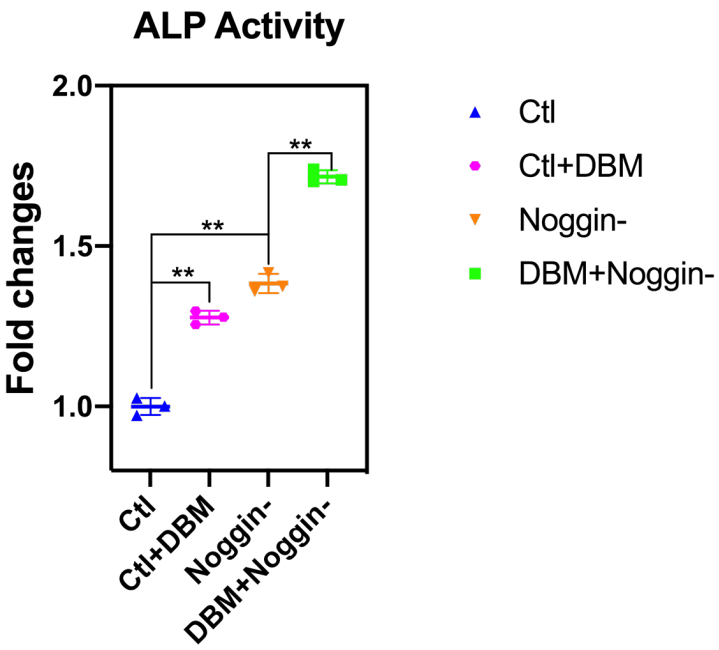
ALP Activity
Fold changes
2.0
1.5
1.0
**
**
**
Ctl
Ctl+DBM
Noggin-
DBM+Noggin-
Ctl
Ctl+DBM
Noggin-
DBM+Noggin-

C

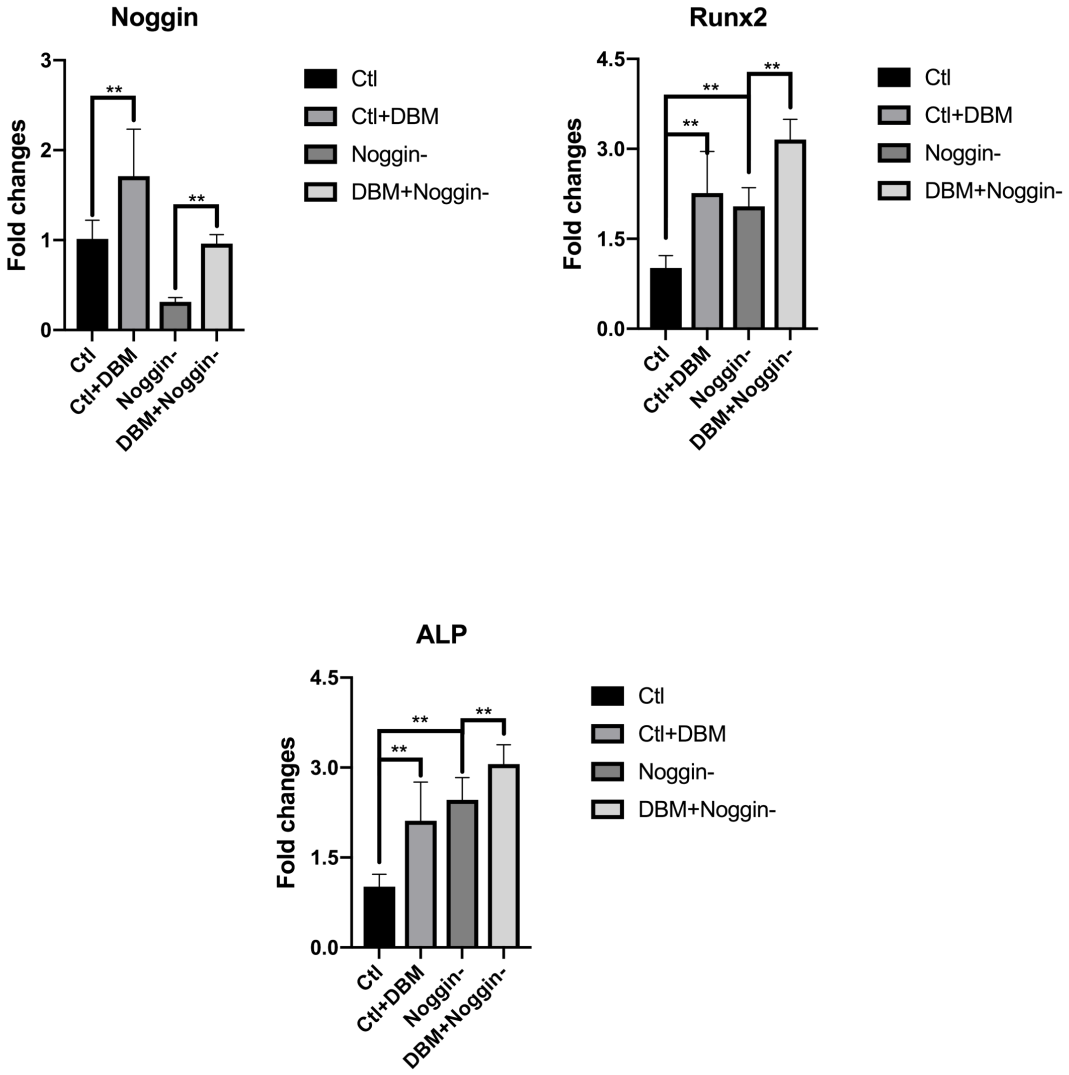

Figure 4.3. DBM and BMSCs were encapsulated in the MeGC hydrogel. The osteogenic differentiation of the BMSCs was evaluated through ALP staining on day 4 and day 7 (A); ALP activity on day 7 (B). The gene expression of Noggin and the specific osteogenic gene markers, including Runx2 and ALP, were also examined by qRT-PCR analysis after 7 days osteogenic induction (C) (**$p<0.05$).

A

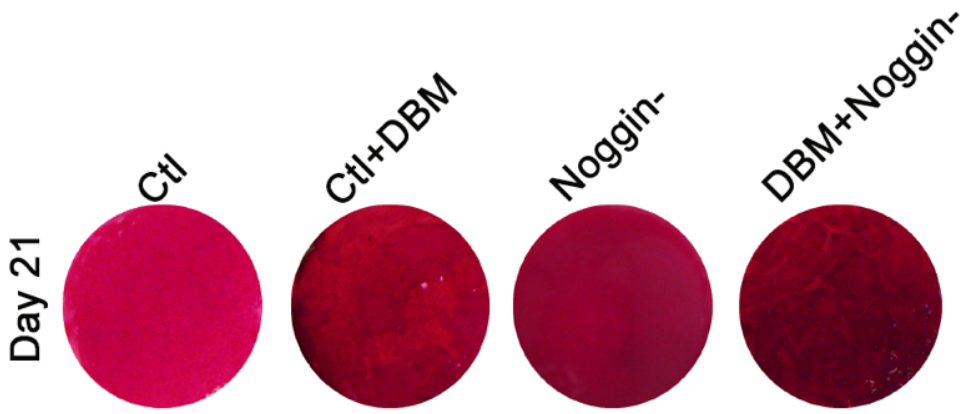

B

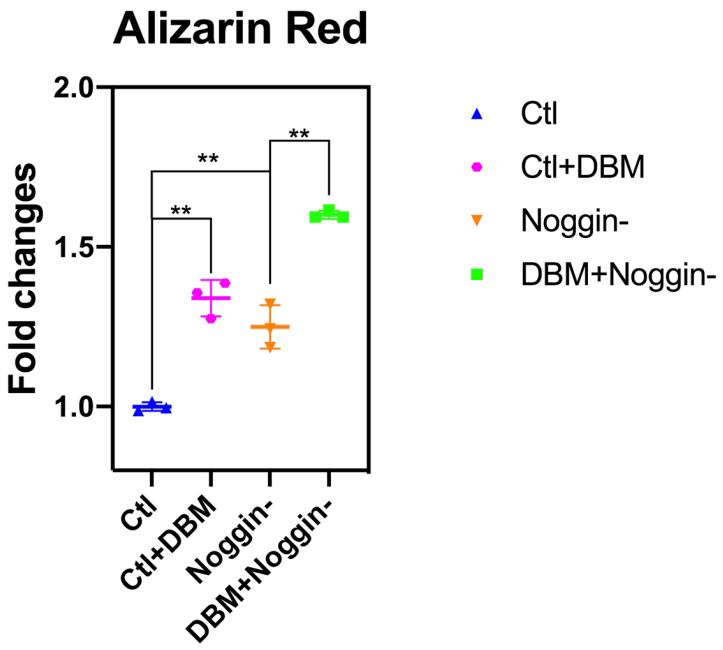

Figure 4.4. Alizarin red S staining (A) and its quantification (B) were employed to detect the calcium deposition in the MeGC hydrogel on day 21 (**p<0.05).

4.4 Heparinization enhances the osteogenesis of BMSCs

Heparinized chitosan (Hep-MeGC) was synthesized by EDC chemically conjugating heparin to the surface of the previous MeGC. The photopolymerizable hydrogel can be initiated by the riboflavin (RF) and cross-linked by the visible blue light. BMSCs, with the concentration of $2x10^6$ cells/ml, were seeded in the MeGC and Hep-MeGC hydrogel, respectively (without DBM), and the osteogenic differentiation of the encapsulated BMSCs was investigated by examining the ALP expression on day 7 and the calcium deposition on day 21. Compared with the MeGC, the Hep-MeGC hydrogel demonstrated a more intensified staining color in both ALP and Alizarin red S staining, which indicated that heparinization enhanced the osteogenesis of the encapsulated BMSCs, even without the application of DBM (Figure 4.5).

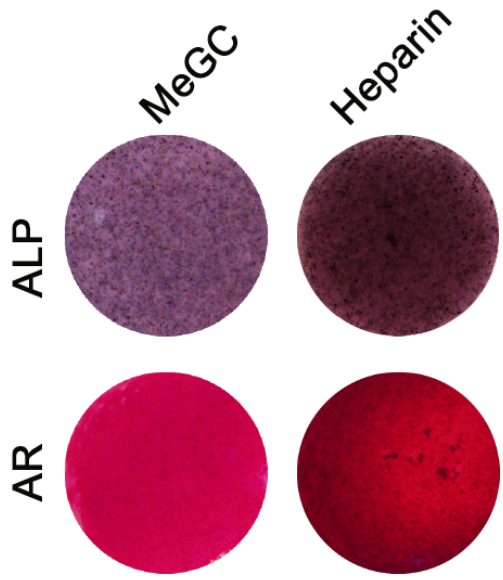

Figure 4.5. BMSCs were encapsulated in MeGC and Hep-MeGC hydrogel, respectively. ALP staining and Alizarin red S staining was conducted on day 7 and day 21.

4.5 BMSCs proliferation in the Hep-MeGC hydrogel with Noggin suppression and DBM

BMSCs and DBM (with 1/1 DBM/hydrogel ratio) were co-encapsulated in the Hep-MeGC hydrogel, and the hydrogels were incubated in the growth medium for 14 days. Live/dead staining was performed on day 1 and day 7 to investigate the morphology changes of the cells. Images showed that both control and Noggin suppression BMSCs congregated and extended spreading along the DBM on day 7 (Figure 4.6A). Alamar blue assay was also employed to characterize the proliferation potential of the cells in the Hep-MeGC hydrogels. The fluorescence intensity kept increasing over 14 days, and the incorporation of DBM further promoted the proliferation of the encapsulated BMSCs compared with the non-treated group (Figure 4.6B).

A

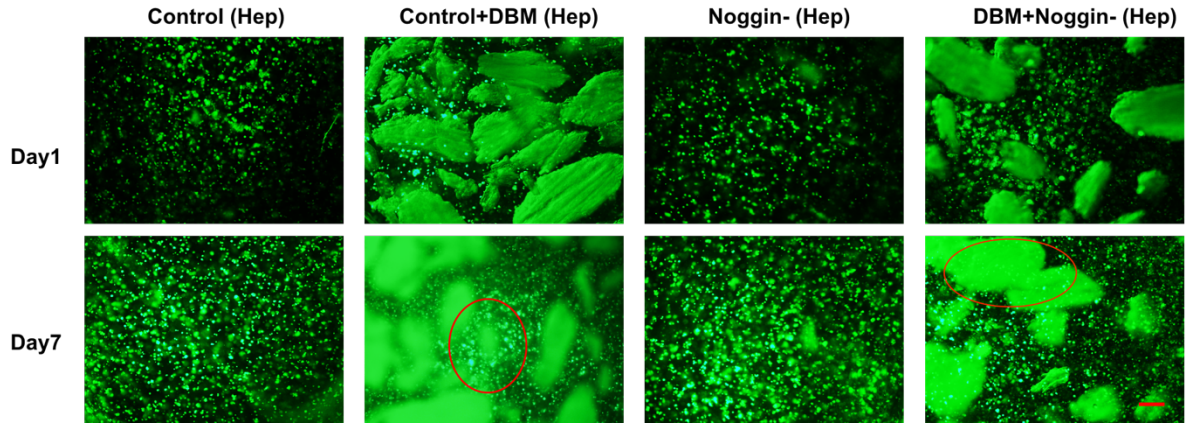

B

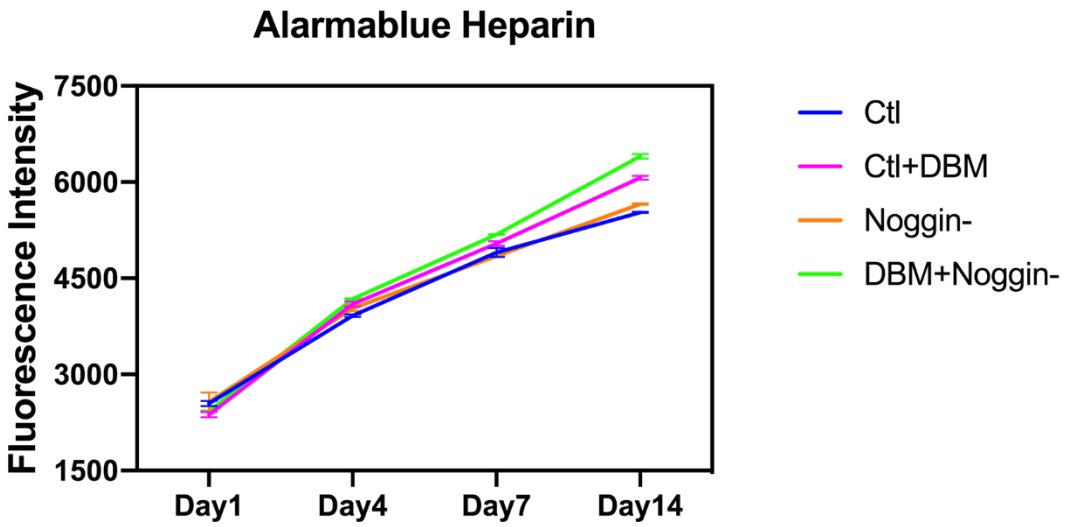

Figure 4.6. BMSCs and DBM were co-encapsulated in the Hep-MeGC hydrogel. Live/dead staining was performed on day 1 and day 7 (A); The fluorescence intensity of Alamar blue was investigated on day 1, day 4, day 7 and day 14 (B) (Scale bar=500 μm).

4.6 Osteogenesis of BMSCs in the Hep-MeGC hydrogel with Noggin-suppression and DBM

The osteogenic differentiation of the encapsulated BMSCs in the Hep-MeGC hydrogel was investigated through ALP staining and its protein activity test on day 4 and day 7. The most intensified color in ALP staining was displayed in Hep-MeGC hydrogels with DBM and Noggin-suppression (Figure 4.7A). With the Noggin-shRNA transduction, the ALP activity was increased to 1.25-fold, and the DBM application extensively enhanced the value to 1.61-fold compared with the non-treated control (Figure 4.7B). qRT-PCR was employed to evaluate the expression of the osteogenic markers on day 7. Noggin suppression and DBM increased the expression of genes, Runx2 and ALP, to 3.03-fold and 2.41-fold, confirming the most potent capacity to enhance the osteogenic differentiation of BMSCs (Figure 4.7C). The backward stage of the osteogenesis was evaluated through Alizarin red S staining and its quantification on day 21. Consistent results showed that the stimulation of DBM in BMSCs enhanced the calcium deposition, which is significantly higher in cells with the transfection of Noggin-shRNA when compared with control (Figure 4.8).

Moreover, when compared with MeGC in parallel, the osteogenic differentiation potential of the encapsulated BMSCs in each group is much higher in the Hep-MeGC hydrogel then that detected in the MeGC as evaluated by the ALP production, ultimate mineralization, and the expression of osteogenic genes. All the results confirmed that heparinization and Noggin-suppression can effectively enhance the osteoinductivity of DBM (Figure 4.3, 4.4, 4.7, 4.8).

A

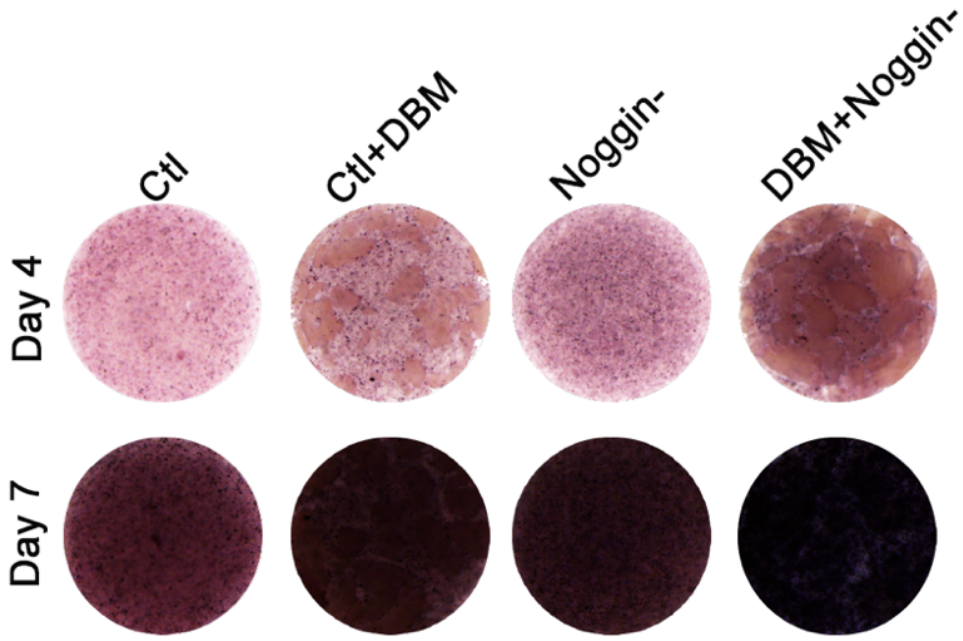
Ctl
Ctl+DBM
Noggin-
DBM+Noggin-
Day 4
Day 7

B

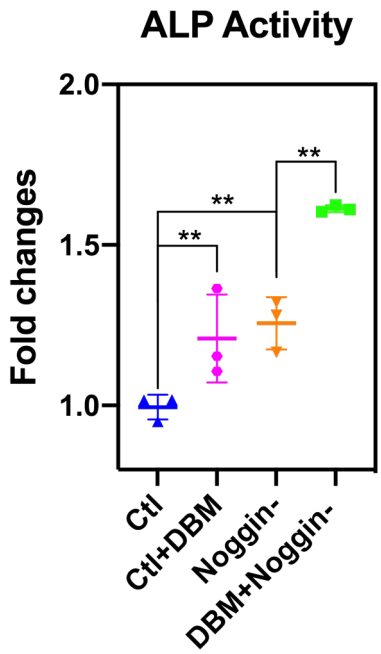
ALP Activity
Fold changes
2.0
1.5
1.0
**
**
**
Ctl
Ctl+DBM
Noggin-
DBM+Noggin-

C

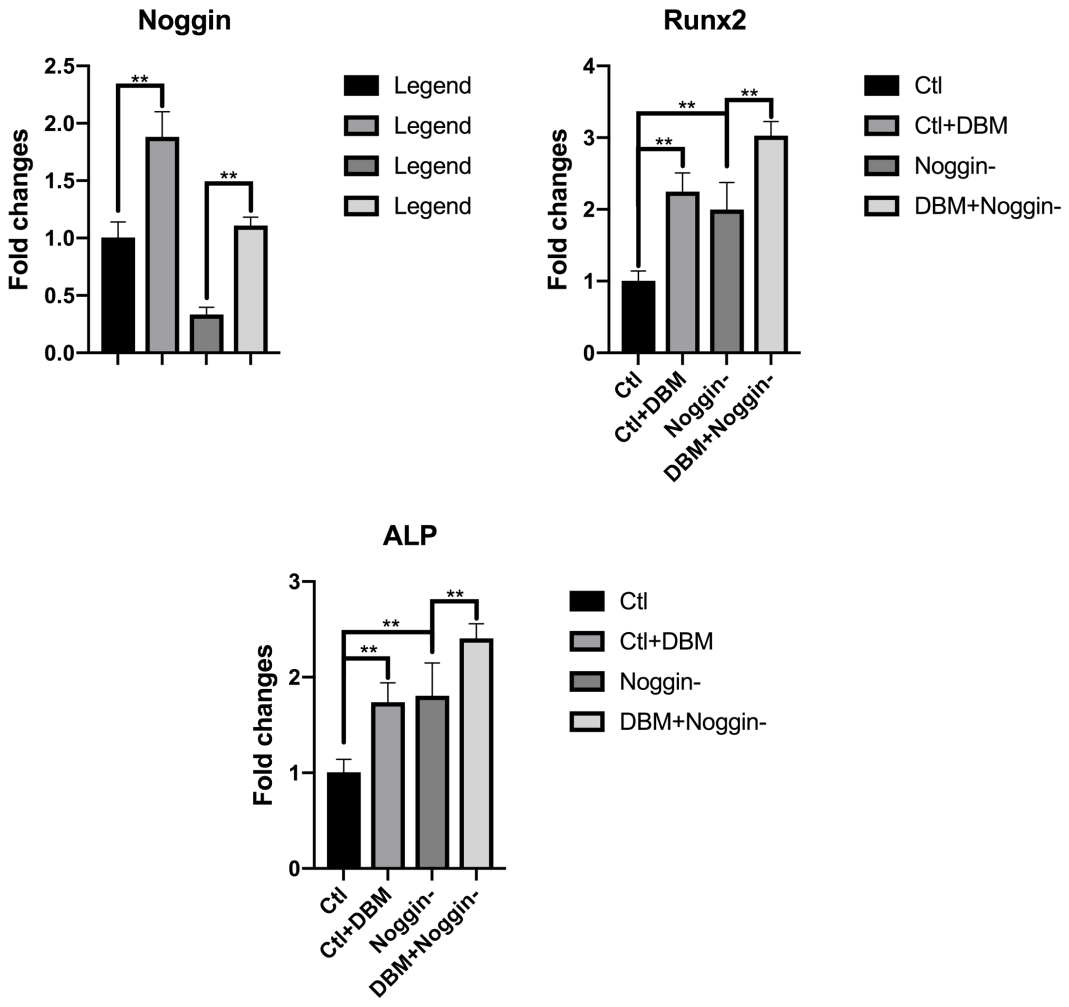

Figure 4.7. BMSCs and DBM were encapsulated in the Hep-MeGC hydrogel. The osteogenic differentiation of the encapsulated cells was evaluated through ALP staining on day 4 and day 7 (A); ALP activity on day 7 (B). qRT-PCR was carried out on day 7 to investigate the RNA expression of Noggin, Runx2, and ALP (C) (**P<0.05).

A

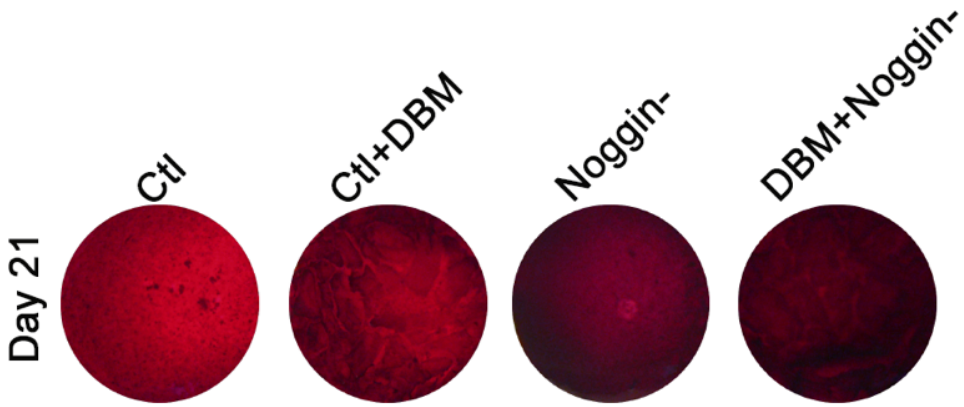

B

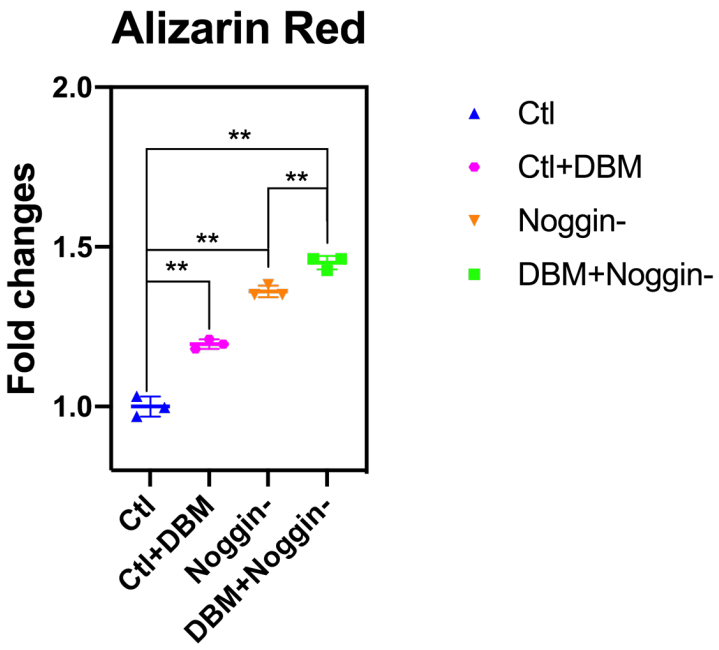

Figure 4.8. BMSCs and DBM were encapsulated in the Hep-MeGC hydrogels. Alizarin red S staining and its quantification were performed on day 21 to determine the calcium deposition (**P<0.05).

Chapter 5

In vivo bone regeneration in critical-sized defect with DBM and Noggin suppression in the Hep-MeGC hydrogel

To investigate the effect of DBM and Noggin suppression in the Hep-MeGC hydrogel on bone regeneration, we further conducted the *in vivo* study by injecting the Hep-MeGC hydrogel loaded with DBM and BMSCs with Noggin suppression to the critical-sized mice calvarial defects (n=6 defects/group). 6 weeks postoperatively, mice were euthanized to collect the bone tissue, and micro-CT was employed for reconstruction to assess the extent of bone healing. Images revealed that the remaining defect size was minimized by the Noggin-suppression and DBM application, indicating the most powerful ability for bone healing (Figure 5.1A). Moreover, to quantify the bone repair, relative bone growth surface area (Bone growth area %), bone volume/tissue volume (BV/TV %) and trabecular number (Tb.N.) were measured, and the original defect size was used to normalize the results. Compared with the non-treated control group (8.58%), the defect with DBM application and Noggin-suppression BMSCs was covered by new bone tissue at 59.78%. BV/TV % and Tb.N. also increased to 3.96% and 0.33 mm-1, respectively, which is notably higher than that of the control (1.37% and 0.11 mm-1) (Figure 5.1B).

The histology section with H & E, Masson Trichrome, and Picrosirius red staining was further employed to evaluate the quality of new bone tissue. Results showed that in the control group, there is only little amount of bone repair at the edge of the defect region, and with DBM and Noggin-suppression, more bone-like tissue was formed to fill the defect. We also confirmed the results by using the immunohistochemistry assay to evaluate the expression of

osteocalcin (OCN), and the most intensified staining was shown in the combinational group, indicating an efficient approach to enhance bone regeneration (Figure 5.2).

A

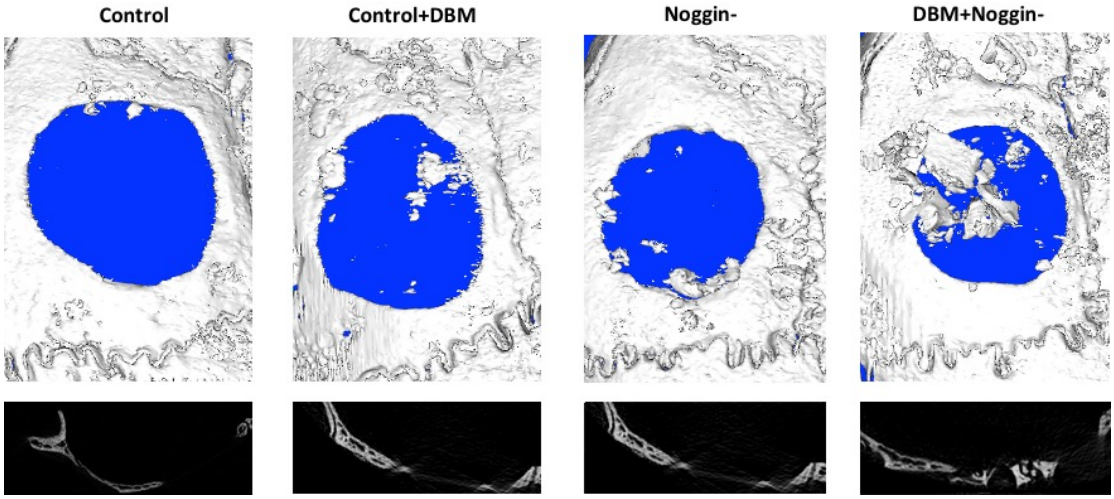

B

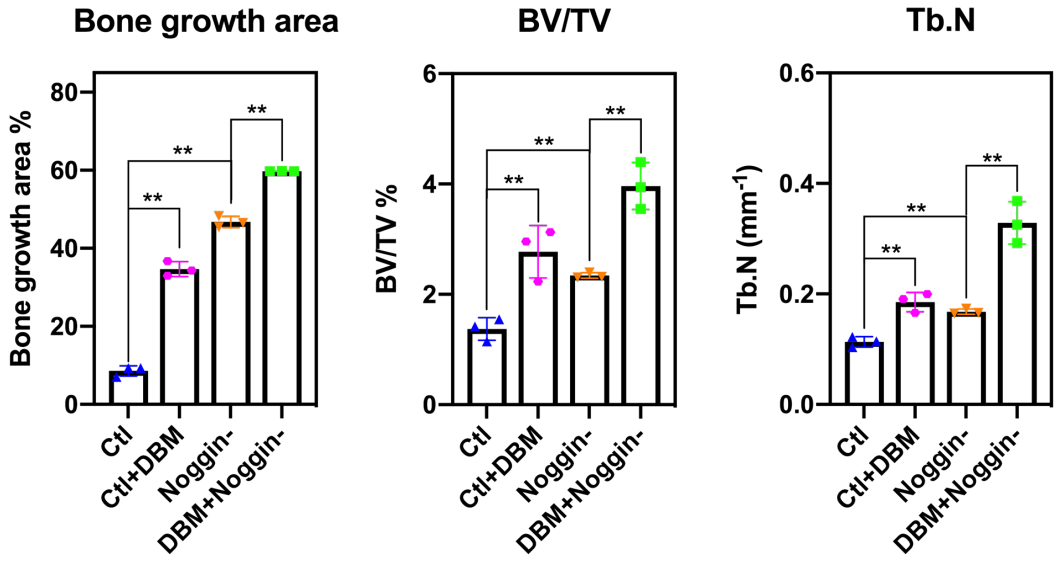

Figure 5.1. DBM and BMSCs were co-encapsulated in the Hep-MeGC hydrogel which was injected to critical-sized (3 x 3 mm) calvarial defects. To evaluate the bone repair, collected

calvarial bone were analyzed through microCT (A) and quantification of relative bone growth surface area (left), bone volume/tissue volume (BV/TV %) (middle) and trabecular number (Tb.N., mm^{-1}) (right) (B). (**P<0.05)

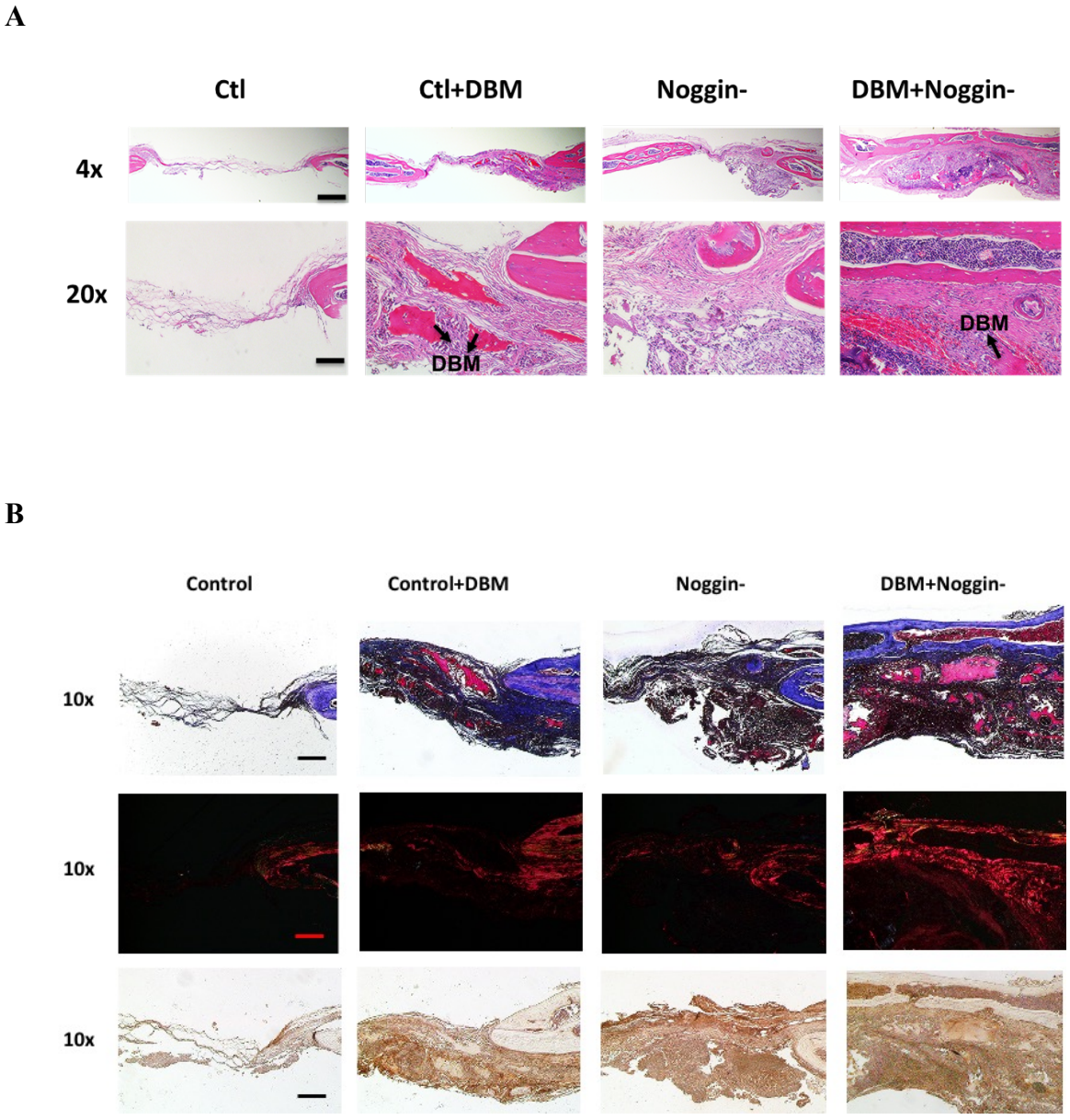

Figure 5.2. After 6 weeks operation, histology section was performed to demonstrate the bone healing. With the Hematoxyline and eosin (H & E) staining (A), Masson trichrome

staining (B) (above) and Picrosirius red staining (B) (middle), the regenerated bone tissue was investigated. The expression of OCN was examined through immunohistochemical staining (B) (below) (Scale bar for 4x=500 μm; Scale bar for 10x=200 μm; Scale bar for 20x=100 μm)

Conclusion

DBM, the allograft bone, of which inorganic mineral has been removed, consists of multiple osteoinductive factors that could modulate the osteogenic differentiation of BMSCs. However, its implementation in bone regeneration for large defects is limited by the rapid dispersion and low osteoinductivity [33]. To overcome these barriers and maximize the osteogenic activity of DBM, this study aims to seek a new method to efficiently enhance the DBM-based bone regeneration by suppressing BMP antagonist and employing the heparinized chitosan hydrogel (Hep-MeGC). Based on the *in vitro* study, Noggin suppression and DBM significantly increased osteogenesis of hBMSCs in Hep-MeGC hydrogels, as shown by increased ALP expression, mineralization, and osteogenic gene expression (Runx2, ALP). The complementary treatment of Noggin suppression + DBM in Hep-MeGC hydrogel further displayed a robust calvarial bone healing *in vivo* as detected by the images/quantification of microCT and the histological/immunohistochemical staining. The mechanistic analysis demonstrated that Noggin suppression increased the osteogenic capacity of DBM through stimulating BMP-Smad signals. Together, we concluded that the incorporation of DBM and Noggin suppression in a biopolymeric Hep-MeGC hydrogel significantly promoted the osteogenesis and increased bone regeneration. Such a complementary strategy built the foundation for further developing translational approaches for potential clinical applications.

Although this work provides a potent concept through which the efficacy of bone repair could be enhanced, the following researches are still necessary for future study. For instance, in this project, Noggin was suppressed in BMSCs by using the lentiviral particles encoding Noggin-shRNA, but there are several constrictions of the lentiviral particles-mediated gene

manipulation. Such a method for gene manipulation may suffer from the immunogenicity issue, and some engineered viruses may reverse to the wild type [60-62]. There is also the possibility to induce insertional mutation with the constitutive expression [61]. In the following work, effective non-viral gene delivery systems, such as the nanoparticle, will be developed and employed to deliver shRNA.

Moreover, hydrogels with self-healing potential will be developed to serve as carriers for DBM. The moldable characteristic can be necessary for clinicians in aiding patients with irregular bone defects. Researches have reported that the laponite-based hydrogel with dendritic molecular binding sites constructs a shape memory and self-healing delivery system for cells and other factors [63, 64]. Therefore, we will fabricate a more practical hydrogel to enhance the osteogenic activity of DBM and increase the efficiency of bone repair.

References

1. Ma, J., et al., *Concise review: cell-based strategies in bone tissue engineering and regenerative medicine.* Stem Cells Transl Med, 2014. **3**(1): p. 98-107.
2. Smrke, D., et al., *Treatment of Bone Defects — Allogenic Platelet Gel and Autologous Bone Technique*, in *Regenerative Medicine and Tissue Engineering*. 2013.
3. Pape, H.C., A. Evans, and P. Kobbe, *Autologous bone graft: properties and techniques.* J Orthop Trauma, 2010. **24 Suppl 1**: p. S36-40.
4. Dupoirieux, L., et al., *Experimental study on demineralized bone matrix (DBM) and coral as bone graft substitutes in maxillofacial surgery.* International Journal of Oral and Maxillofacial Surgery, 1994. **23**(6, Part 2): p. 395-398.
5. Zhang, M., R.M. Powers, Jr., and L. Wolfinbarger, Jr., *Effect(s) of the demineralization process on the osteoinductivity of demineralized bone matrix.* J Periodontol, 1997. **68**(11): p. 1085-92.
6. Han, B., B. Tang, and M.E. Nimni, *Quantitative and sensitive in vitro assay for osteoinductive activity of demineralized bone matrix.* J Orthop Res, 2003. **21**(4): p. 648-54.
7. Guerra, M.F., et al., *Rim versus sagittal mandibulectomy for the treatment of squamous cell carcinoma: two types of mandibular preservation.* Head Neck, 2003. **25**(12): p. 982-9.
8. Shariatinia, Z., *Pharmaceutical applications of chitosan.* Advances in Colloid and Interface Science, 2019. **263**: p. 131-194.

9. Ravi Kumar, M.N.V., *A review of chitin and chitosan applications.* Reactive and Functional Polymers, 2000. **46**(1): p. 1-27.

10. Gazzerro, E., V. Gangji, and E. Canalis, *Bone morphogenetic proteins induce the expression of noggin, which limits their activity in cultured rat osteoblasts.* The Journal of clinical investigation, 1998. **102**(12): p. 2106-2114.

11. Capdevila, J. and R.L. Johnson, *Endogenous and ectopic expression of noggin suggests a conserved mechanism for regulation of BMP function during limb and somite patterning.* Dev Biol, 1998. **197**(2): p. 205-17.

12. Zimmerman, L.B., J.M. De Jesus-Escobar, and R.M. Harland, *The Spemann organizer signal noggin binds and inactivates bone morphogenetic protein 4.* Cell, 1996. **86**(4): p. 599-606.

13. Zhao, Y., et al., *The osteogenic effect of bone morphogenetic protein-2 on the collagen scaffold conjugated with antibodies.* J Control Release, 2010. **141**(1): p. 30-7.

14. Burge, R., et al., *Incidence and Economic Burden of Osteoporosis-Related Fractures in the United States, 2005–2025.* Journal of Bone and Mineral Research, 2007. **22**(3): p. 465-475.

15. Paderni, S., S. Terzi, and L. Amendola, *Major bone defect treatment with an osteoconductive bone substitute.* Chir Organi Mov, 2009. **93**(2): p. 89-96.

16. Kim, W.S., et al., *Bone defect repair with tissue-engineered cartilage.* Plast Reconstr Surg, 1994. **94**(5): p. 580-4.

17. Zhao, Y., et al., *Crosslinked three-dimensional demineralized bone matrix for the adipose-derived stromal cell proliferation and differentiation.* Tissue Eng Part A, 2009. **15**(1): p. 13-21.

18. Pittenger, M.F., et al., *Multilineage potential of adult human mesenchymal stem cells.* Science, 1999. **284**(5411): p. 143-7.

19. Liu, G., et al., *In vitro and in vivo evaluation of osteogenesis of human umbilical cord blood-derived mesenchymal stem cells on partially demineralized bone matrix.* Tissue Eng Part A, 2010. **16**(3): p. 971-82.

20. Goldberg, V.M. and S. Akhavan, *Biology of Bone Grafts*, in *Bone Regeneration and Repair: Biology and Clinical Applications*, J.R. Lieberman and G.E. Friedlaender, Editors. 2005, Humana Press: Totowa, NJ. p. 57-65.

21. Fillingham, Y. and J. Jacobs, *Bone grafts and their substitutes.* The Bone & Joint Journal, 2016. **98-B**(1_Supple_A): p. 6-9.

22. Aspenberg, P. and T. Turek, *BMP-2 for intramuscular bone induction: effect in squirrel monkeys is dependent on implantation site.* Acta Orthop Scand, 1996. **67**(1): p. 3-6.

23. Rosenthal, R.K., J. Folkman, and J. Glowacki, *Demineralized bone implants for nonunion fractures, bone cysts, and fibrous lesions.* Clin Orthop Relat Res, 1999(364): p. 61-9.

24. Alom, N., et al., *Bone extracellular matrix hydrogel enhances osteogenic differentiation of C2C12 myoblasts and mouse primary calvarial cells.* J Biomed Mater Res B Appl Biomater, 2018. **106**(2): p. 900-908.

25. Wildemann, B., et al., *Quantification of various growth factors in different demineralized bone matrix preparations.* Journal of Biomedical Materials Research Part A, 2007. **81A**(2): p. 437-442.

26. Holt, D.J. and D.W. Grainger, *Demineralized bone matrix as a vehicle for delivering endogenous and exogenous therapeutics in bone repair.* Advanced Drug Delivery Reviews, 2012. **64**(12): p. 1123-1128.

27. Rabie, A.B., *Vascular endothelial growth pattern during demineralized bone matrix induced osteogenesis.* Connect Tissue Res, 1997. **36**(4): p. 337-45.

28. Jang, C.H., et al., *Mastoid obliteration using a hyaluronic acid gel to deliver a mesenchymal stem cells-loaded demineralized bone matrix: An experimental study.* International Journal of Pediatric Otorhinolaryngology, 2008. **72**(11): p. 1627-1632.

29. Burkus, J.K., et al., *Anterior Lumbar Interbody Fusion Using rhBMP-2 With Tapered Interbody Cages.* Clinical Spine Surgery, 2002. **15**(5): p. 337-349.

30. Chen, N.-F., et al., *Symptomatic ectopic bone formation after off-label use of recombinant human bone morphogenetic protein-2 in transforaminal lumbar interbody fusion.* 2010. **12**(1): p. 40.

31. Perri, B., et al., *Adverse swelling associated with use of rh-BMP-2 in anterior cervical discectomy and fusion: a case study.* The Spine Journal, 2007. **7**(2): p. 235-239.

32. Cahill, K.S., et al., *Prevalence, Complications, and Hospital Charges Associated With Use of Bone-Morphogenetic Proteins in Spinal Fusion Procedures.* JAMA, 2009. **302**(1): p. 58-66.

33. Chesmel, K.D., et al., *Healing response to various forms of human demineralized bone matrix in athymic rat cranial defects.* Journal of Oral and Maxillofacial Surgery, 1998. **56**(7): p. 857-863.

34. Shehadi, J.A. and S.M. Elzein, *Review of commercially available demineralized bone matrix products for spinal fusions: A selection paradigm.* Surgical neurology international, 2017. **8**: p. 203-203.

35. Gruskin, E., et al., *Demineralized bone matrix in bone repair: History and use.* Advanced Drug Delivery Reviews, 2012. **64**(12): p. 1063-1077.

36. Maisani, M., et al., *Cellularizing hydrogel-based scaffolds to repair bone tissue: How to create a physiologically relevant micro-environment?* J Tissue Eng, 2017. **8**: p. 2041731417712073.

37. Tommasi, G., S. Perni, and P. Prokopovich, *An Injectable Hydrogel as Bone Graft Material with Added Antimicrobial Properties.* Tissue Eng Part A, 2016. **22**(11-12): p. 862-72.

38. Bhattarai, N., J. Gunn, and M. Zhang, *Chitosan-based hydrogels for controlled, localized drug delivery.* Adv Drug Deliv Rev, 2010. **62**(1): p. 83-99.

39. Hu, J., et al., *Visible light crosslinkable chitosan hydrogels for tissue engineering.* Acta Biomater, 2012. **8**(5): p. 1730-8.

40. Park, H., et al., *Injectable chitosan hyaluronic acid hydrogels for cartilage tissue engineering.* Acta Biomater, 2013. **9**(1): p. 4779-86.

41. Amsden, B.G., et al., *Methacrylated Glycol Chitosan as a Photopolymerizable Biomaterial.* Biomacromolecules, 2007. **8**(12): p. 3758-3766.

42. Tian, M., et al., *Delivery of demineralized bone matrix powder using a thermogelling chitosan carrier.* Acta Biomaterialia, 2012. **8**(2): p. 753-762.

43. Kim, S., et al., *Photocrosslinkable chitosan hydrogels functionalized with the RGD peptide and phosphoserine to enhance osteogenesis.* J Mater Chem B, 2016. **4**(31): p. 5289-5298.

44. Kim, S., et al., *Design of hydrogels to stabilize and enhance bone morphogenetic protein activity by heparin mimetics.* Acta Biomater, 2018. **72**: p. 45-54.

45. Capila, I. and R.J. Linhardt, *Heparin–Protein Interactions.* Angewandte Chemie International Edition, 2002. **41**(3): p. 390-412.

46. Takada, T., et al., *Sulfated polysaccharides enhance the biological activities of bone morphogenetic proteins.* J Biol Chem, 2003. **278**(44): p. 43229-35.

47. Huber, E., et al., *(*) Demineralized Bone Matrix as a Carrier for Bone Morphogenetic Protein-2: Burst Release Combined with Long-Term Binding and Osteoinductive Activity Evaluated In Vitro and In Vivo.* Tissue Eng Part A, 2017. **23**(23-24): p. 1321-1330.

48. Kuo, W.-J., M.A. Digman, and A.D. Lander, *Heparan sulfate acts as a bone morphogenetic protein coreceptor by facilitating ligand-induced receptor hetero-oligomerization.* Molecular biology of the cell, 2010. **21**(22): p. 4028-4041.

49. Ruppert, R., E. Hoffmann, and W. Sebald, *Human Bone Morphogenetic Protein 2 Contains a Heparin-Binding Site which Modifies Its Biological Activity.* European Journal of Biochemistry, 1996. **237**(1): p. 295-302.

50. Gazzerro, E., V. Gangji, and E. Canalis, *Bone morphogenetic proteins induce the expression of noggin, which limits their activity in cultured rat osteoblasts.* J Clin Invest, 1998. **102**(12): p. 2106-14.

51. Fan, J., et al., *Enhanced Osteogenesis of Adipose-Derived Stem Cells by Regulating Bone Morphogenetic Protein Signaling Antagonists and Agonists.* Stem Cells Transl Med, 2016. **5**(4): p. 539-51.

52. Wan, D.C., et al., *Noggin suppression enhances in vitro osteogenesis and accelerates in vivo bone formation.* J Biol Chem, 2007. **282**(36): p. 26450-9.

53. Fan, J., et al., *Enhanced osteogenesis of adipose derived stem cells with Noggin suppression and delivery of BMP-2.* PLoS One, 2013. **8**(8): p. e72474.

54. James, A.W., et al., *Estrogen/estrogen receptor alpha signaling in mouse posterofrontal cranial suture fusion.* PLoS One, 2009. **4**(9): p. e7120.

55. Fan, J., et al., *Small molecule-mediated tribbles homolog 3 promotes bone formation induced by bone morphogenetic protein-2.* Sci Rep, 2017. **7**(1): p. 7518.

56. Cui, Z.-K., et al., *Simultaneous delivery of hydrophobic small molecules and siRNA using Sterosomes to direct mesenchymal stem cell differentiation for bone repair.* Acta Biomaterialia, 2017. **58**: p. 214-224.

57. Pietrzak, W.S., J. Woodell-May, and N. McDonald, *Assay of bone morphogenetic protein-2, -4, and -7 in human demineralized bone matrix.* J Craniofac Surg, 2006. **17**(1): p. 84-90.

58. Hollinger, J.O., H. Uludag, and S.R. Winn, *Sustained release emphasizing recombinant human bone morphogenetic protein-2.* Adv Drug Deliv Rev, 1998. **31**(3): p. 303-318.

59. Erickson, D.M., et al., *Recombinant bone morphogenetic protein (BMP)-2 regulates costochondral growth plate chondrocytes and induces expression of BMP-2 and BMP-4 in a cell maturation-dependent manner.* J Orthop Res, 1997. **15**(3): p. 371-80.

60. Davis, S.S., *Biomedical applications of nanotechnology--implications for drug targeting and gene therapy.* Trends Biotechnol, 1997. **15**(6): p. 217-24.

61. Welm, B.E., et al., *Lentiviral transduction of mammary stem cells for analysis of gene function during development and cancer.* Cell Stem Cell, 2008. **2**(1): p. 90-102.

62. Sahoo, S.K., S. Parveen, and J.J. Panda, *The present and future of nanotechnology in human health care.* Nanomedicine, 2007. **3**(1): p. 20-31.

63. Tamesue, S., et al., *Linear versus dendritic molecular binders for hydrogel network formation with clay nanosheets: studies with ABA triblock copolyethers carrying guanidinium ion pendants.* J Am Chem Soc, 2013. **135**(41): p. 15650-5.

64. Wang, Q., et al., *High-water-content mouldable hydrogels by mixing clay and a dendritic molecular binder.* Nature, 2010. **463**(7279): p. 339-43.